Electronic Supplementary Material (ESI) for CrystEngComm.

Testing the limits of halogen bonding in coordination chemistry

Mladen Borovina, Ivan Kodrin, Marijana Đaković*

Department of Chemistry, Faculty of Science, University of Zagreb, Zagreb, Croatia

Supplementary information

Table of Contents

1. Single crystal X-ray crystallography 3
2. Powder X-ray crystallography 13

1. Single crystal X-ray crystallography

Table S1. Crystal data and details of the structure determination for **1a–7b.**

Compound	**1a**	**1b**	**2a**	**2b**
Formula	$C_{20}H_{22}CoCl_2N_2O_4$	$C_{20}H_{22}NiCl_2N_2O_4$	$C_{20}H_{22}CoBr_2N_2O_4$	$C_{20}H_{22}NiBr_2N_2O_4$
M_r	484.22	484.00	573.14	572.92
Colour and habit	dark orange, block	Clear blue, block	dark orange, block	dark blue, prism
Crystal system, space group	Triclinic, *P*-1	Triclinic, *P*-1	Triclinic, *P*-1	Monoclinic, $P\ 2_1/n$
Crystal dimensions (mm^3)	0.32x0.24x0.20	0.25x0.25x0.18	0.27x0.25x0.18	0.32x0.16x0.13
a (Å)	9.0807(5)	9.1894(2)	6.4978(5)	7.9966(5)
b (Å)	10.2369(6)	9.9870(3)	8.8500(7)	9.5422(7)
c (Å)	13.0194(8)	13.4819(5)	10.3960(5)	15.2152(8)
α (˚)	74.910(5)	73.422(3)	100.254(5)	90
β (˚)	74.027(5)	71.424(3)	101.706(5)	97.623(6)
γ (˚)	86.362(5)	85.191(2)	99.895(7)	90
V ($Å^3$)	1123.37(12)	1124.05(6)	562.47(7)	1150.74(13)
Z	2	2	1	2
D_{calc} (g cm^{-3})	1.432	1.430	1.692	1.653
μ (mm^{-1})	1.029	1.128	4.342	4.342
F(000)	498	500	285	572
θ range for data collection (˚)	4.37 – 26.00	4.26 – 28.00	4.27 – 26.00	4.48 – 25.99
h,k,l range	-9:11, -12:12, -16:16	-12:12, -13:13, -17:17	-8:6, -10:10, -11:12	-9:9, -11:10, -18:8
Scan type	ω	ω	ω	ω
No. measured reflections	9149	19684	4189	4420
No. independent reflections (R_{int})	4395 (0.0189)	4487 (0.0211)	1820 (0.0468)	1505 (0.0306)
No. observed reflections, $I \geq 2\sigma(I)$	3549	5409	2194	2243
No. refined parameters	269	269	135	135
R, wR [$I \geq 2\sigma(I)$]	0.0341, 0.0829	0.0336, 0.0830	0.0358, 0.0794	0.0463, 0.1076
R, wR [all data]	0.0459, 0.0890	0.0438, 0.0882	0.0468, 0.0851	0.0812, 0.1204
Goodness of fit on F^2, S	1.027	1.041	1.079	1.027
Max., min. electron density (e $Å^{-3}$)	0.273, -0.304	0.274, -0.279	0.566, -0.660	0.824, -0.573
CCDC number	1582547	1582539	1582550	1582538

Compound	**3a**	**3b**	**4a**	**4b**
Formula	$C_{20}H_{22}CoI_2N_2O_4$	$C_{20}H_{22}NiI_2N_2O_4$	$C_{18}H_{20}CoCl_2N_4O_4$	$C_{18}H_{20}NiCl_2N_4O_4$
M_r	667.12	666.90	486.21	485.99
Colour and habit	Orange, prism	Blue, prism	Orange, block	Light blue, plate
Crystal system, space group	Monoclinic, $P\ 2_1/n$	Monoclinic, $P\ 2_1/n$	Triclinic, P-1	Triclinic, P-1
Crystal dimensions (mm^3)	0.18x0.08x0.07	0.27x0.11x0.1	0.23x0.21x0.1	0.17x0.09x0.03
a (Å)	7.9717(5)	8.0225(2)	6.3162(4)	6.3212(5)
b (Å)	9.7058(4)	9.6265(2)	8.8584(8)	8.9502(7)
c (Å)	15.4552(5)	15.4896(3)	10.1891(5)	10.0197(8)
α (˚)	90	90	99.706(6)	100.977(7)
β (˚)	96.710(4)	96.406(2)	101.645(5)	100.919(7)
γ (˚)	90	90	100.278(7)	99.073(6)
V ($Å^3$)	1187.60(10)	1188.77(5)	536.88(7)	535.27(8)
Z	2	2	1	1
D_{calc} (g cm^{-3})	1.866	1.863	1.504	1.508
μ (mm^{-1})	3.348	3.439	1.079	1.187
F(000)	642	644	249	250
θ range for data collection (˚)	4.41 – 27.00	4.42 – 27.00	4.35 – 27.99	4.15 – 26.00
h,k,l range	-9:10, -7:12, -18:19	-10:10, -12:12, -19:19	-8:8, -11:9, -13:13	-7:7, -9:11, -12:12
Scan type	ω	ω	ω	ω
No. measured reflections	5140	28298	4382	4103
No. independent reflections (R_{int})	2583 (0.0232)	2594 (0.0333)	2587(0.0228)	2100(0.0221)
No. observed reflections, $I \geq 2\sigma(I)$	1993	2291	2288	1803
No. refined parameters	135	135	135	135
R, wR [$I \geq 2\sigma(I)$]	0.0423, 0.1073	0.0352, 0.0881	0.0364, 0.0926	0.0388, 0.0813
R, wR [all data]	0.0576, 0.1168	0.0407, 0.0921	0.0428, 0.0977	0.0498, 0.0859
Goodness of fit on F^2, S	1.066	1.067	1.075	1.061
Max., min. electron density (e $Å^{-3}$)	0.551, -0.1024	0.669, -1.319	0.335, -0.475	0.306, -0.258
CCDC number	1582542	1582540	1582548	1582545

Compound	**5a**	**5b**	**6a**	**6b**	**7a**
Formula	$C_{18}H_{20}CoBr_2N_4O_4$	$C_{18}H_{20}NiBr_2N_4O_4$	$C_{18}H_{20}CoI_2N_4O_4$	$C_{18}H_{20}NiI_2N_4O_4$	$C_{18}H_{20}CoBr_2N_4O_4$
M_r	575.13	574.91	669.11	668.89	575.13
Colour and habit	Dark orange, block	Light blue, prism	Dark orange, block	Light blue, block	Light orange, plate
Crystal system, space group	Triclinic, *P-1*	Triclinic, *P-1*	Triclinic, *P-1*	Triclinic, *P-1*	Triclinic, *P-1*
Crystal dimensions (mm^3)	0.35x0.23x0.19	0.2x0.06x0.04	0.22x0.21x0.19	0.21x0.18x0.15	0.21x0.15x0.07
a (Å)	6.3290(5)	6.3344(4)	6.3513(9)	6.3490(3)	6.1501(4)
b (Å)	8.9473(6)	9.0280(8)	9.2560(11)	9.2589(5)	8.7162(7)
c (Å)	10.2742(7)	10.1145(7)	10.3631(8)	10.2457(4)	10.7960(8)
α (˚)	100.396(6)	101.295(7)	102.241(8)	102.659(4)	100.733(6)
β (˚)	101.149(7)	100.541(6)	100.737(9)	100.162(4)	97.813(6)
γ (˚)	100.044(6)	99.102(7)	98.708(11)	98.163(4)	101.437(6)
V ($Å^3$)	548.09(7)	546.23(7)	573.27(12)	568.11(5)	548.26(7)
Z	1	1	1	1	1
D_{calc} (g cm^{-3})	1.742	1.748	1.938	1.955	1.742
μ (mm^{-1})	4.459	4.576	3.471	3.601	4.457
F(000)	285	286	321	322	285
θ range for data collection (˚)	4.34 – 27.00	4.14 – 27.00	4.27 – 26.00	4.15 – 27.00	4.25 – 26.00
h,k,l range	-7:8, -11:11, -13:13	-8:5, -11:11, -12:12	-7:7, -11:11, -11:12	-8:8, -9:11, -13:13	-7:7, -10:10, -13:13
Scan type	ω	ω	ω	ω	ω
No. measured reflections	4340	4386	4009	4563	4740
No. independent reflections (R_{int})	2373(0.0179)	2375 (0.0148)	2226(0.0244)	2476(0.0177)	2153 (0.0223)
No. observed reflections, $I \geq 2\sigma(I)$	1893	1970	1748	2139	1782
No. refined parameters	135	135	135	135	135
R, wR [$I \geq 2\sigma(I)$]	0.0354, 0.0807	0.0312, 0.0632	0.0329, 0.0765	0.0287, 0.0623	0.0330, 0.0770
R, wR [all data]	0.0490, 0.0864	0.0415, 0.0675	0.0467, 0.0848	0.0349, 0.0662	0.0439, 0.0818
Goodness of fit on F^2, S	1.032	1.037	1.046	1.065	1.052
Max., min. electron density (e $Å^{-3}$)	0.503, -0.558	0.622, -0.590	0.564, -0.954	0.580, -0.911	0.265, -0.439
CCDC number	1582546	1582541	1582549	1582543	1582544

Table S2. Selected bond distances (Å) and angles (°) for **1a** and **1b.**

	1a	**1b**
M1–O1	2.030(1)	2.012(1)
M1–O2	2.036(2)	2.018(1)
M2-O3	2.030(1)	2.009(1)
M2-O4	2.038(2)	2.017(1)
M1–N1	2.192(2)	2.126(1)
M2-N2	2.205(2)	2.134(1)
O1–M1–O2	89.53(6)	91.57(5)
O1–M1–O2^{i}	90.47(6)	88.43(5)
O1–M1–N1	91.59(6)	88.72(5)
O2–M1–N1	91.99(7)	92.03(6)
O1–M1–N1^{i}	88.41(6)	91.28(5)
O2–M1–N1^{i}	88.01(7)	87.97(6)
O3–M2–O4	89.06(6)	91.33(6)
O3–M2–O4^{ii}	90.94(6)	88.67(6)
O3–M2–N2	86.67(6)	87.33(5)
O4–M2–N2	89.83(6)	90.55(6)
O3–M2–N2^{ii}	93.34(6)	92.67(5)
O4–M2–N2^{ii}	90.17(6)	89.45(6)

Symmetry codes (i): –x, -y+1, -z+2; (ii): –x+1, -y+1, -z+1. M = Co(II) (**1a**), Ni(II) (**1b**).

Table S3. Selected bond distances (Å) and angles (°) for **2a–7a**.

	2a	**2b**	**3a**	**3b**
M1–O1	2.014(2)	2.007(3)	2.019(3)	2.011(2)
M1–O2	2.043(2)	2.018(3)	2.042(3)	2.027(2)
M1–N1	2.233(2)	2.120(4)	2.188(4)	2.121(3)
O1–M1–O2	89.67(9)	91.69(12)	90.29(12)	91.94(9)
O1–M1–O2^{i}	90.33(9)	88.30(12)	89.71(12)	88.06(9)
O1–M1–N1	89.78(9)	89.30(13)	89.29(13)	89.41(10)
O2–M1–N1	91.79(9)	91.61(12)	92.06(12)	91.57(10)
O1–M1–N1^{i}	90.22(9)	90.70(13)	90.71(13)	90.59(10)
O2–M1–N1^{i}	88.21(9)	88.38(12)	87.94(12)	88.43(10)
	4a	**4b**	**5a**	**5b**
M1–O1	2.011(1)	1.998(2)	2.015(2)	2.005(2)
M1–O2	2.029(1)	2.007(2)	2.030(2)	2.012(2)
M1–N1	2.246(2)	2.171(2)	2.245(2)	2.172(2)
O1–M1–O2	89.85(6)	91.77(7)	89.90(8)	91.64(7)
O1–M1–O2^{i}	90.15(6)	88.23(7)	90.10(8)	88.36(7)
O1–M1–N1	90.55(6)	89.50(7)	89.67(8)	90.47(7)
O2–M1–N1	87.22(6)	92.26(7)	92.54(8)	87.97(7)
O1–M1–N1^{i}	89.45(6)	90.50(7)	90.33(8)	89.53(7)
O2–M1–N1^{i}	92.78(6)	87.74(7)	87.46(8)	92.03(7)
	6a	**6b**	**7a**	
M1–O1	2.018(2)	1.998(2)	2.016(2)	
M1–O2	2.026(3)	2.014(2)	2.034(2)	
M1–N1	2.233(3)	2.169(2)	2.236(2)	
O1–M1–O2	89.91(11)	91.76(9)	89.51(8)	
O1–M1–O2^{i}	90.08(11)	88.24(9)	90.49(8)	
O1–M1–N1	90.34(11)	89.65(9)	91.82(8)	
O2–M1–N1	88.64(12)	91.30(9)	85.87(8)	
O1–M1–N1^{i}	89.66(11)	90.35(9)	88.18(8)	
O2–M1–N1^{i}	91.36(12)	88.70(9)	94.13(8)	

Symmetry codes (i): -x+1, -y+1, -z+1. M = Co(II) (**2a–7a**), Ni(II) (**2b–6b**).

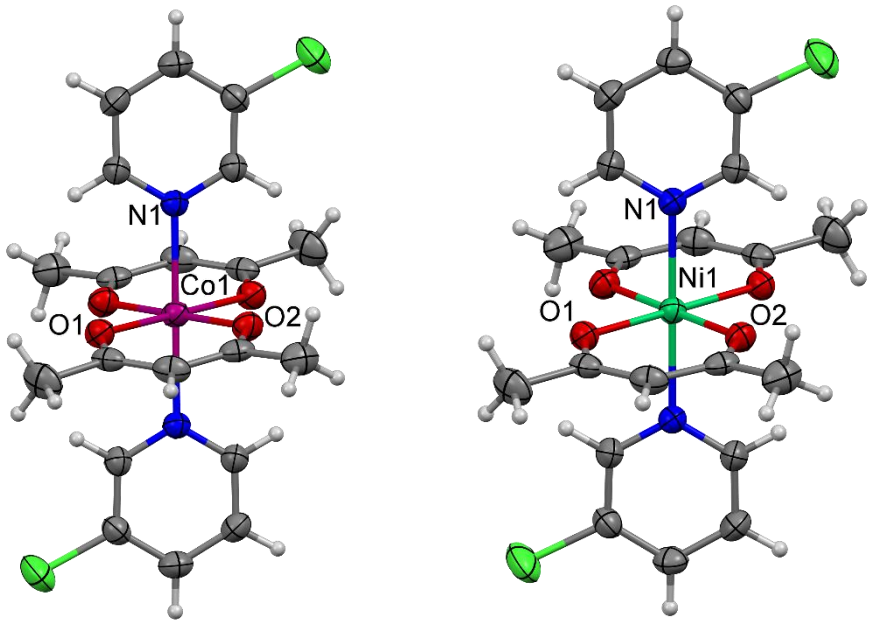

(a) **(b)**

Figure S1. ORTEP-style plot of (a) $[Co(acac)_2(3\text{-}Clpy)_2]$ **(1a)** and (b) $[Ni(acac)_2(3\text{-}Clpy)_2]$ **(1b)** with partial labeling scheme. Thermal ellipsoids are drawn at 30% probability level at 296(2) K.

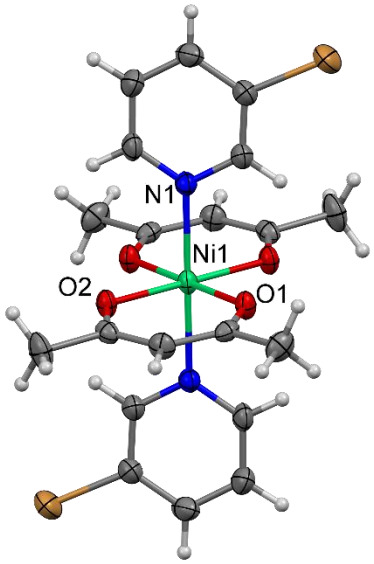

Figure S2. ORTEP-style plot of $[Ni(acac)_2(3\text{-}Brpy)_2]$ **(2b)** with partial labeling scheme. Thermal ellipsoids are drawn at 30% probability level at 296(2) K.

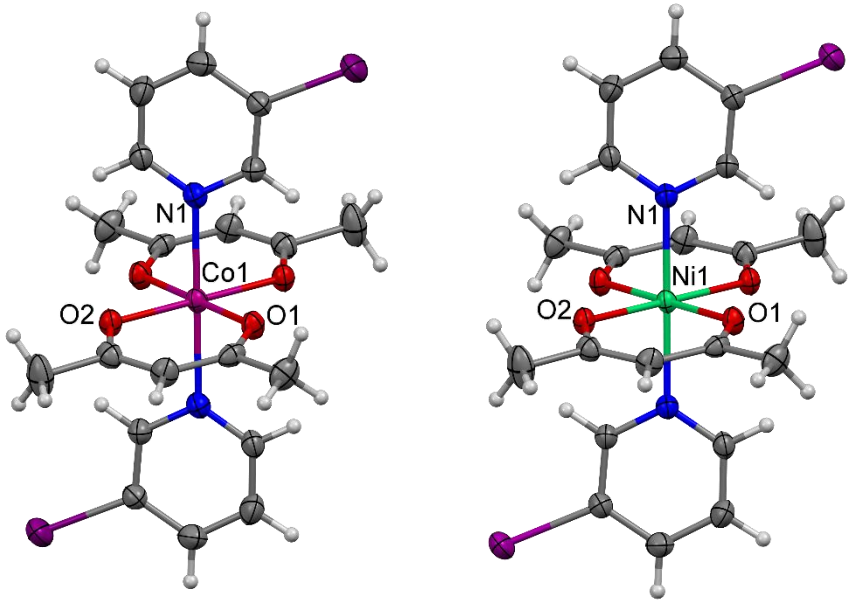

(a) **(b)**

Figure S3. ORTEP-style plot of (a) $[Co(acac)_2(3\text{-Ipy})_2]$ **(3a)** and (b) $[Ni(acac)_2(3\text{-Ipy})_2]$ **(3b)** with partial labeling scheme. Thermal ellipsoids are drawn at 30% probability level at 296(2) K.

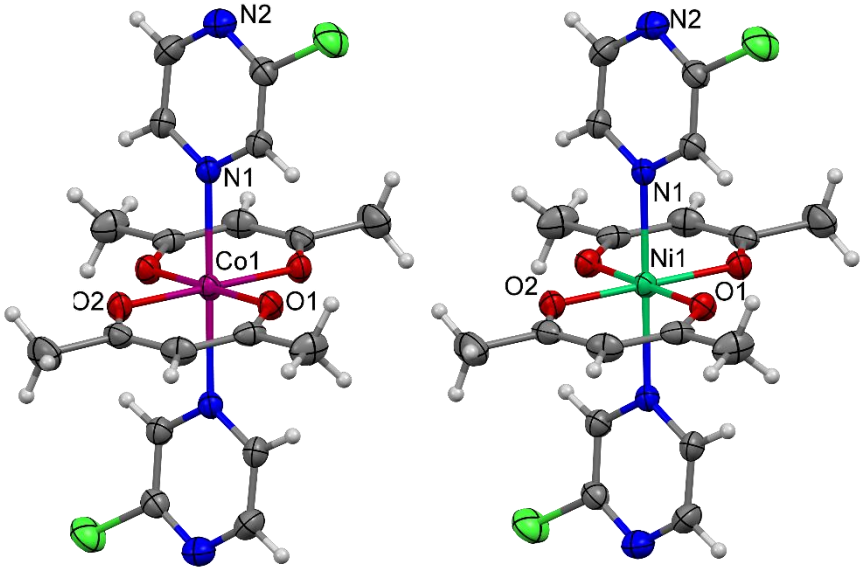

(a) **(b)**

Figure S4. ORTEP-style plot of (a) $[Co(acac)_2(2\text{-Clpz})_2]$ **(4a)** and (b) $[Ni(acac)_2(2\text{-Clpz})_2]$ **(4b)** with partial labeling scheme. Thermal ellipsoids are drawn at 30% probability level at 296(2) K.

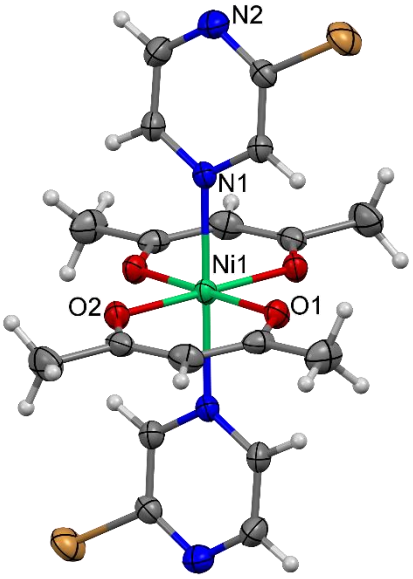

Figure S5. ORTEP-style plot of $[Ni(acac)_2(2\text{-}Brpz)_2]$ **(5b)** with partial labeling scheme. Thermal ellipsoids are drawn at 30% probability level at 296(2) K

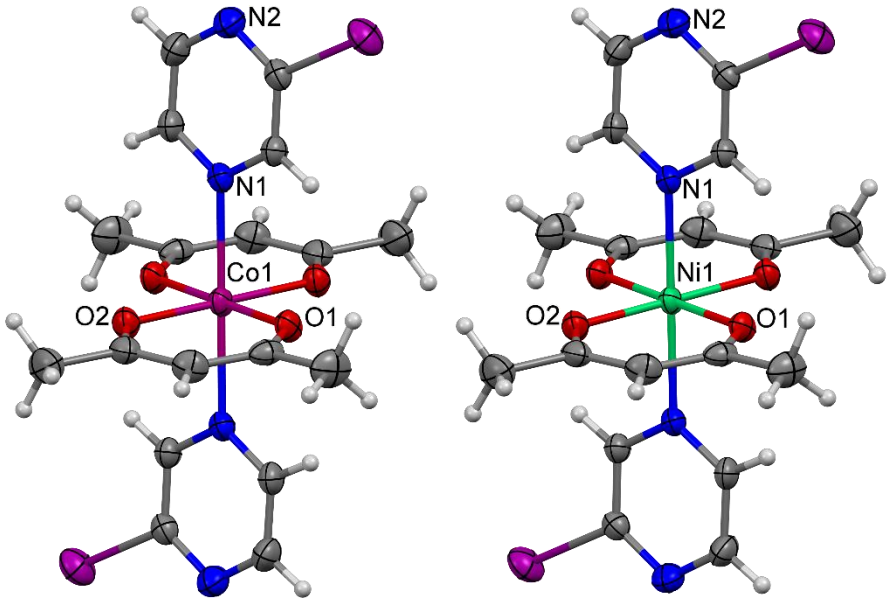

(a) **(b)**

Figure S6. ORTEP-style plot of (a) $[Co(acac)_2(2\text{-}Ipz)_2]$ **(6a)** and (b) $[Ni(acac)_2(2\text{-}Ipz)_2]$ **(6b)** with partial labeling scheme. Thermal ellipsoids are drawn at 30% probability level at 296(2) K

Secondary interactions in the crystal packing of 1a–7a.

In all crystal structures (**1a**–**7a**) stacking interactions were observed but they do delicately adopt to different types of primary interactions that were identified.

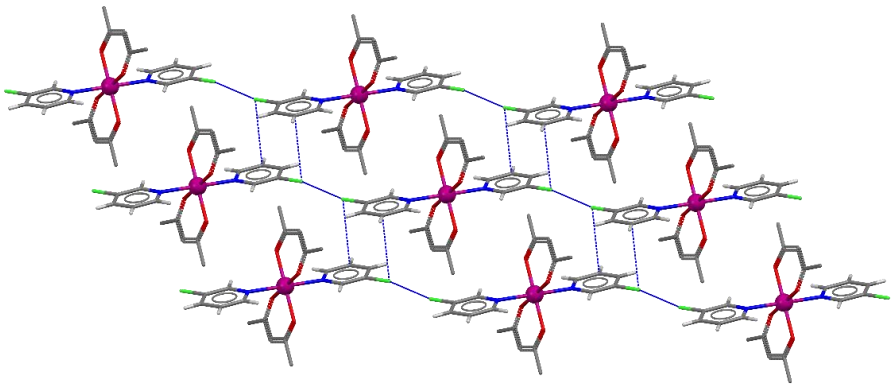

Figure S7. The 1-D chains, formed via type I Cl···Cl contacts in **1a**, are further extended into 2-D layers through stacking interactions. The corresponding nickel(II) complex, $[Ni(acac)_2(3\text{-}Clpy)_2]$ (**1b**), is isostructural with **1a**. Hydrogen atoms on the acac ligands are omitted for clarity.

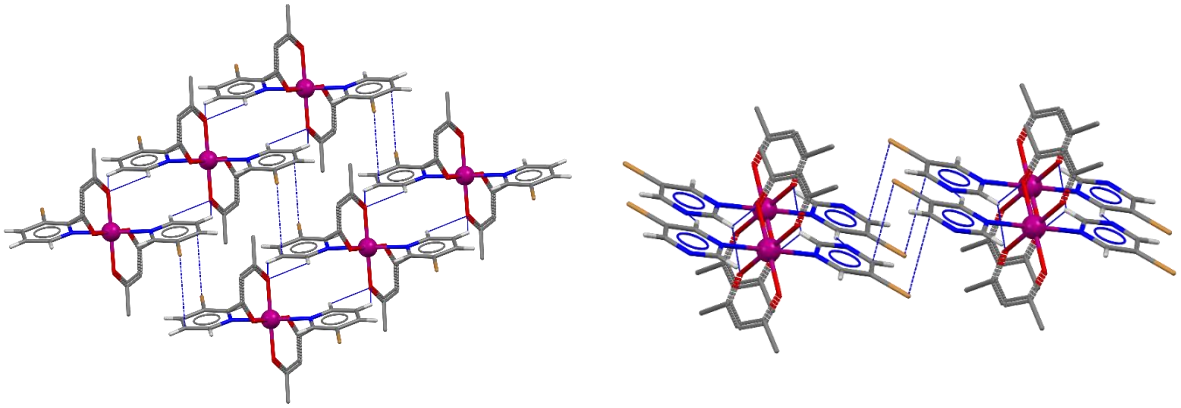

(a) (b)

Figure S8. (a) Stacking interactions in $[Co(acac)_2(3\text{-}Brpy)_2]$ (**2a**). 1-D strands formed via primary C–H···O hydrogen-bond interactions are further extended into 2-D layers through stacking interactions. The corresponding pyrazine complexes (**4a**–**6b**) are isostructural with **2a**. (b) Stacking interactions in $[Co(acac)_2(5\text{-}Brpm)_2]$ (**7a**), 1-D strands formed via primary C–H···O and C–H···N hydrogen-bond interactions are further extended into 2-D layers through stacking. Hydrogen atoms on the acac ligands are omitted for clarity.

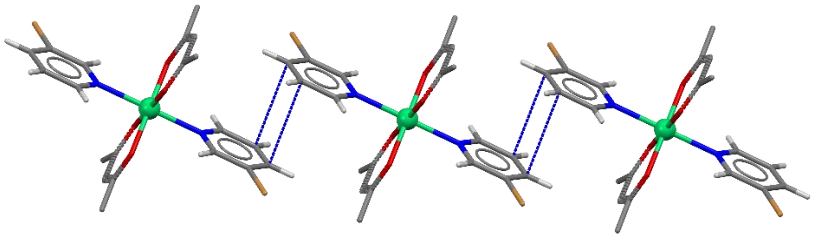

Figure S9, π-stacking between the neighbouring molecules of [Ni(acac)$_2$(3-Brpy)$_2$] (**2b**), isostructural with **3a** and **3b,** extends in 1-D chains.

Table S4 Details on π···π geometry for **1a–7a**.

	Ring	α	β	Cg···Cg	CgI_Perp	Slippage
1a	Cg(1)···Cg(1)^{i}	0.02(11)	37.9	4.367(1)	3.446(1)	2.682
1b	Cg(1)···Cg(1)^{i}	0.02(10)	35.7	4.322(1)	3.510(1)	2.522
2a	Cg(2)···Cg(2)^{ii}	0.02(17)	41.3	4.999(2)	3.756(1)	3.299
2b	Cg(2)···Cg(2)^{iii}	0.0(2)	31.7	4.127(3)	3.510(1)	2.171
3a	Cg(2)···Cg(2)^{iii}	0.0(2)	31.4	4.074(3)	3.476(2)	2.124
3b	Cg(2)···Cg(2)^{iii}	0.00(18)	32.6	4.133(2)	3.481(1)	2.228
4a	Cg(3)···Cg(3)^{iv}	0	39.8	4.658(1)	3.580(1)	2.980
4b	Cg(3)···Cg(3)^{ii}	0.00(14)	39.8	4.653(2)	3.576(1)	2.978
5a	Cg(3)···Cg(3)^{ii}	0.03(17)	40.3	4.790(2)	3.653(1)	3.098
5b	Cg(3)···Cg(3)^{iv}	0.04(14)	40.3	4.786(2)	3.650(1)	3.096
6a	Cg(3)···Cg(3)^{ii}	0.0(2)	40.8	4.974(2)	3.768(1)	3.248
6b	Cg(3)···Cg(3)^{iv}	0.02(16)	41.0	4.995(1)	3.769(1)	3.278
7a	Cg(3)···Cg(3)^{iv}	0.03(16)	45.9	5.321(1)	3.705(1)	3.819

Symmetry codes: (i): 1–x, 2–y, 1–z; (ii): 1–x, 1–y, 2–z; (iii): 1–x, –y, 1–z; (iv): 1–x, 1–y, –z.
Cg(1): N2, C11-C15; Cg(2): N1, C1-C5; Cg(3): N1, N2, C1-C4.

2. Powder X-ray crystallography

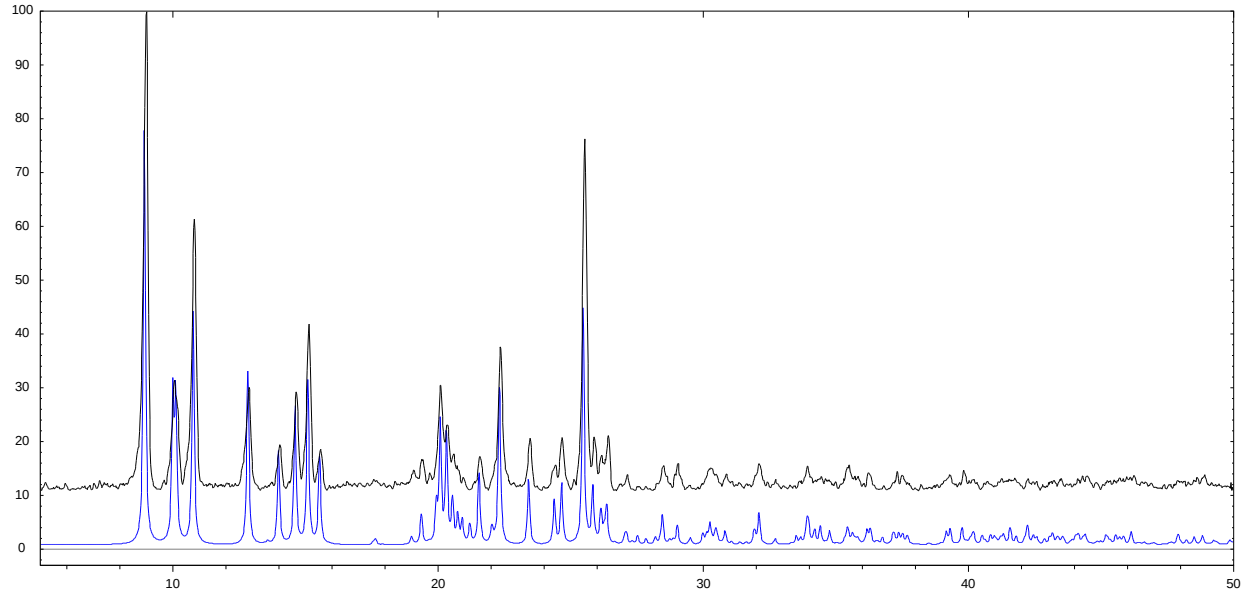

Figure S10. Experimental (**black**) and calculated (**blue**) PXRD traces of $[Co(acac)_2(3\text{-}Clpy)_2]$ (**1a**)

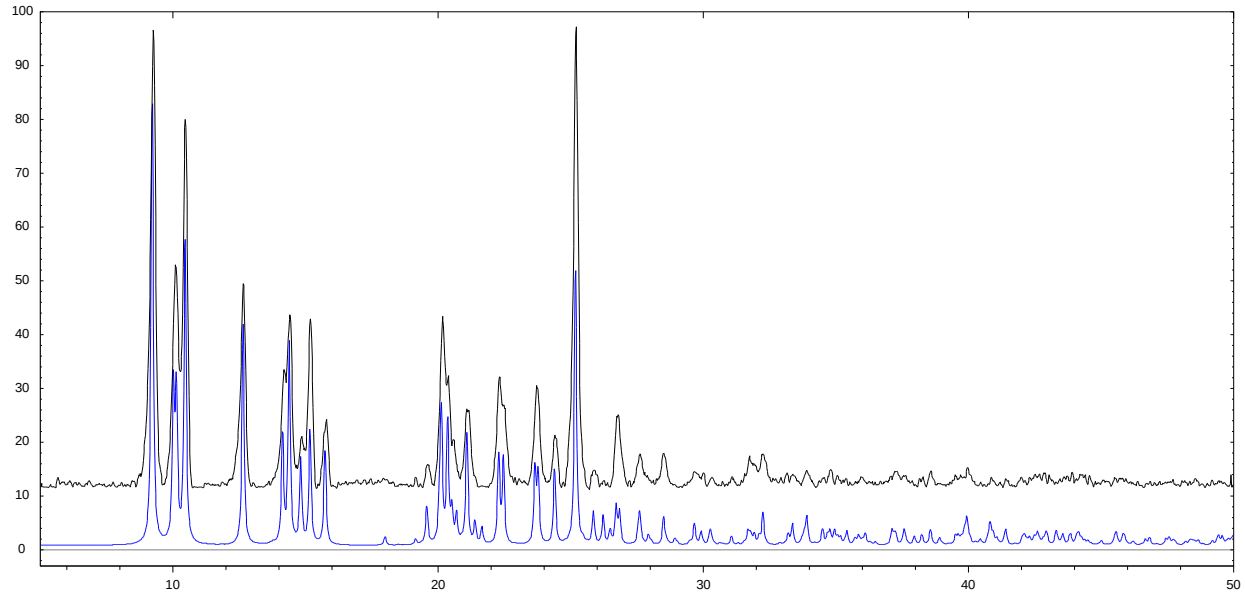

Figure S11. Experimental (**black**) and calculated (**blue**) PXRD traces of $[Ni(acac)_2(3\text{-}Clpy)_2]$ (**1b**)

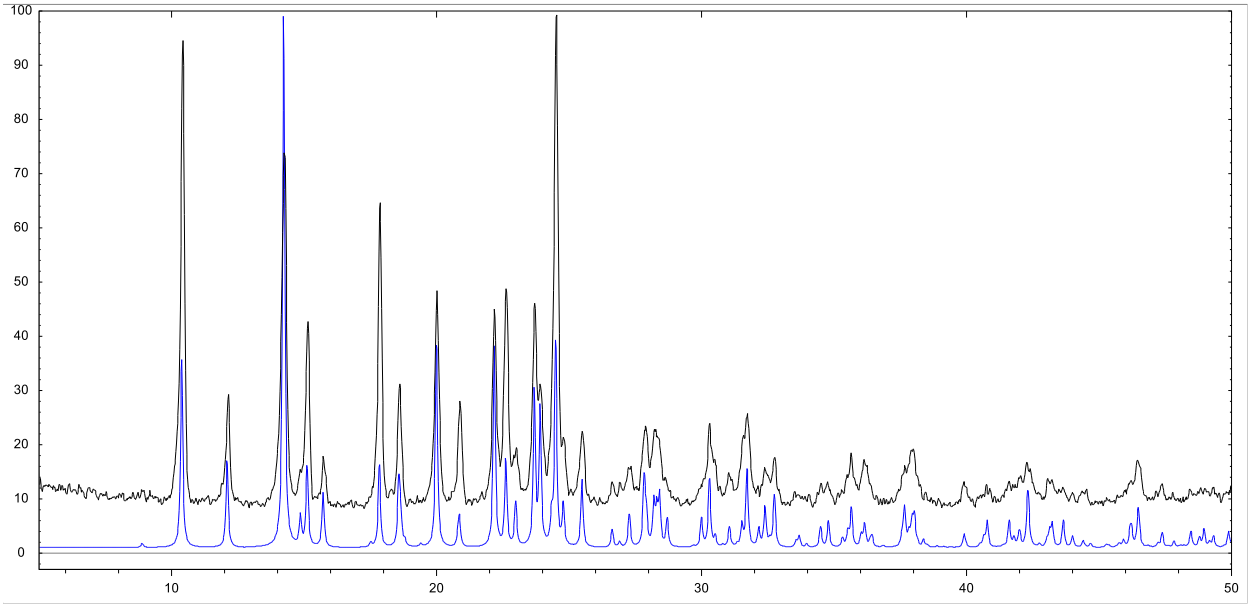

Figure S12. Experimental (**black**) and calculated (**blue**) PXRD traces of $[Co(acac)_2(3\text{-}Brpy)_2]$ (**2a**)

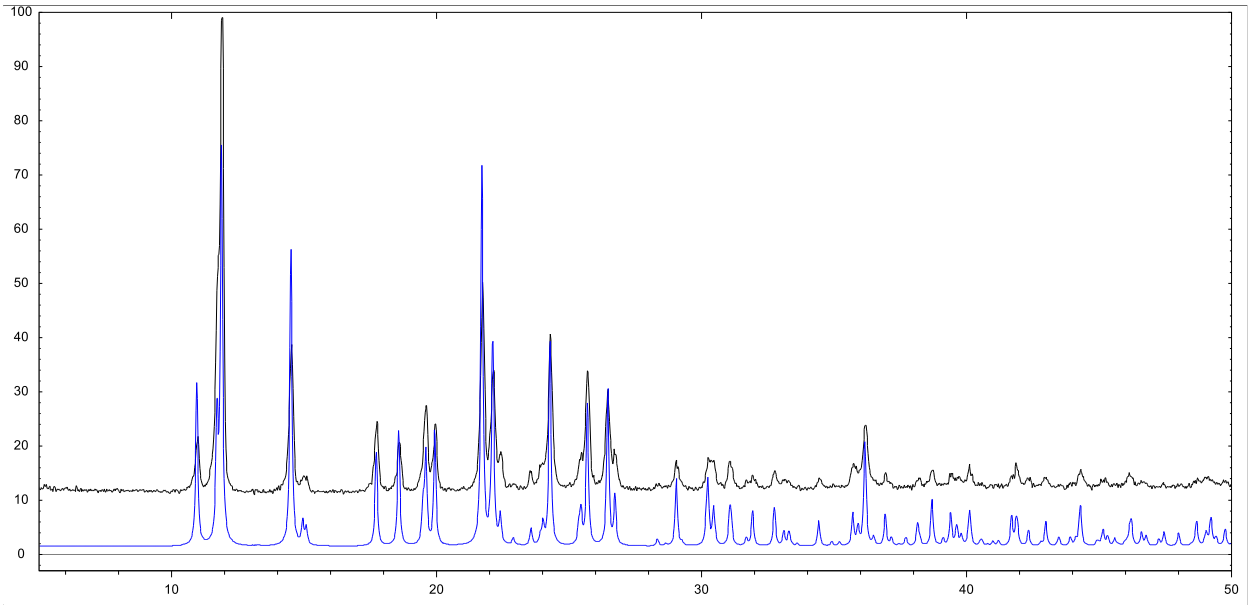

Figure S13. Experimental (**black**) and calculated (**blue**) PXRD traces of $[Ni(acac)_2(3\text{-}Brpy)_2]$ (**2b**)

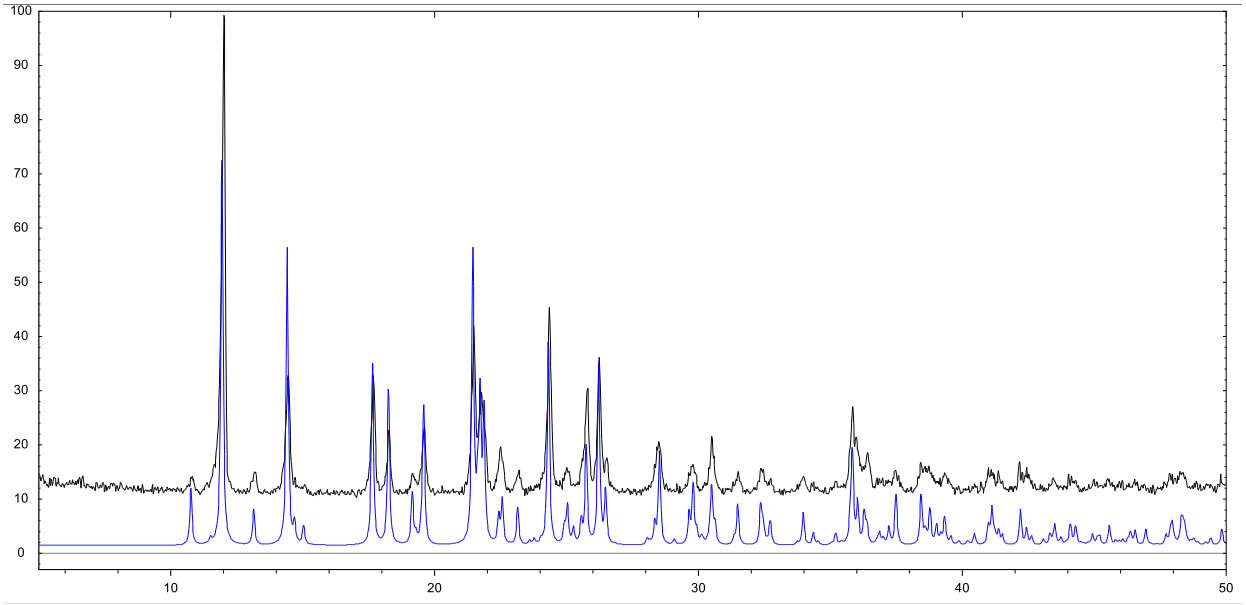

Figure S14. Experimental (**black**) and calculated (**blue**) PXRD traces of $[Co(acac)_2(3\text{-}Ipy)_2]$ (**3a**)

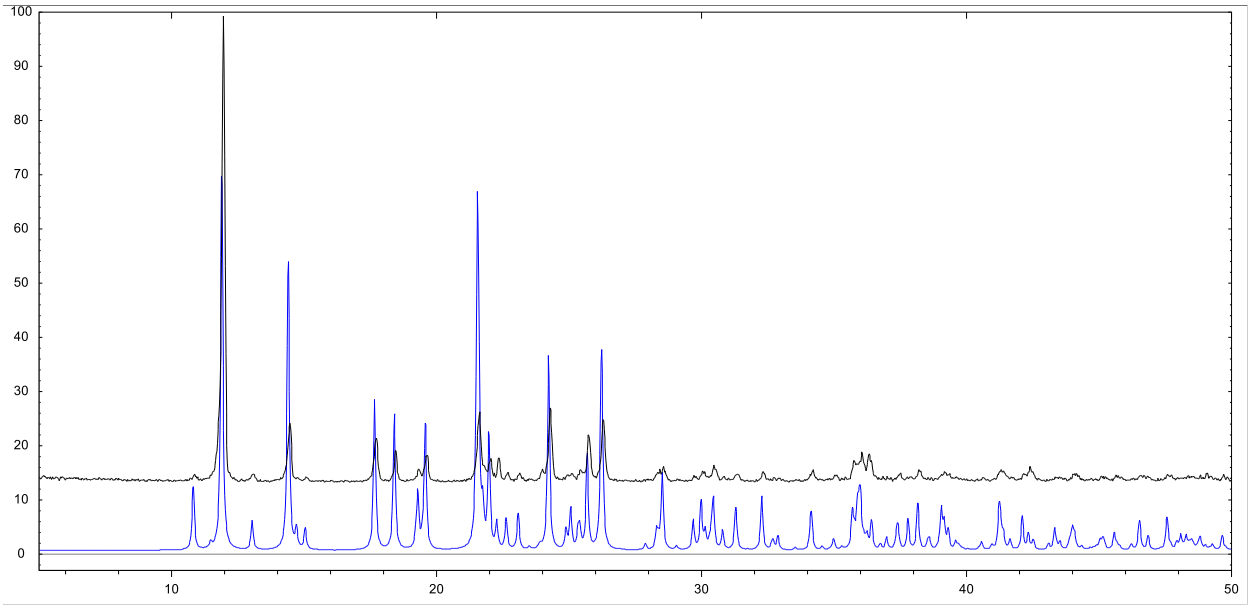

Figure S15. Experimental (**black**) and calculated (**blue**) PXRD traces of $[Ni(acac)_2(3\text{-}Ipy)_2]$ (**3b**)

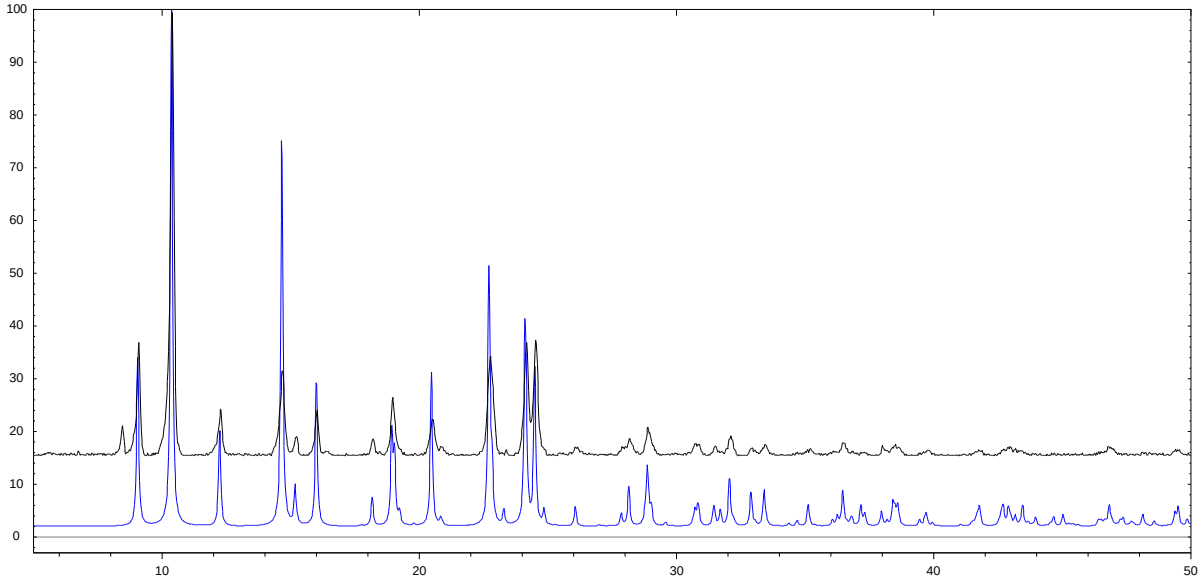

Figure S16. Experimental (**black**) and calculated (**blue**) PXRD traces of $[Co(acac)_2(2\text{-}Clpz)_2]$ (**4a**)

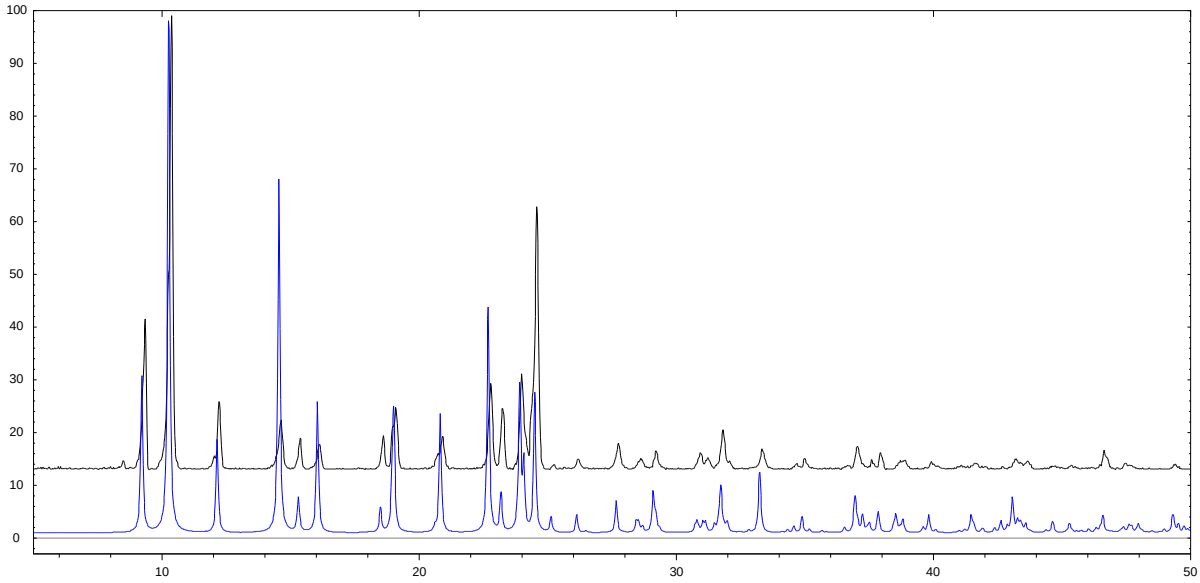

Figure S17. Experimental (**black**) and calculated (**blue**) PXRD traces of $[Ni(acac)_2(2\text{-}Clpz)_2]$ (**4b**)

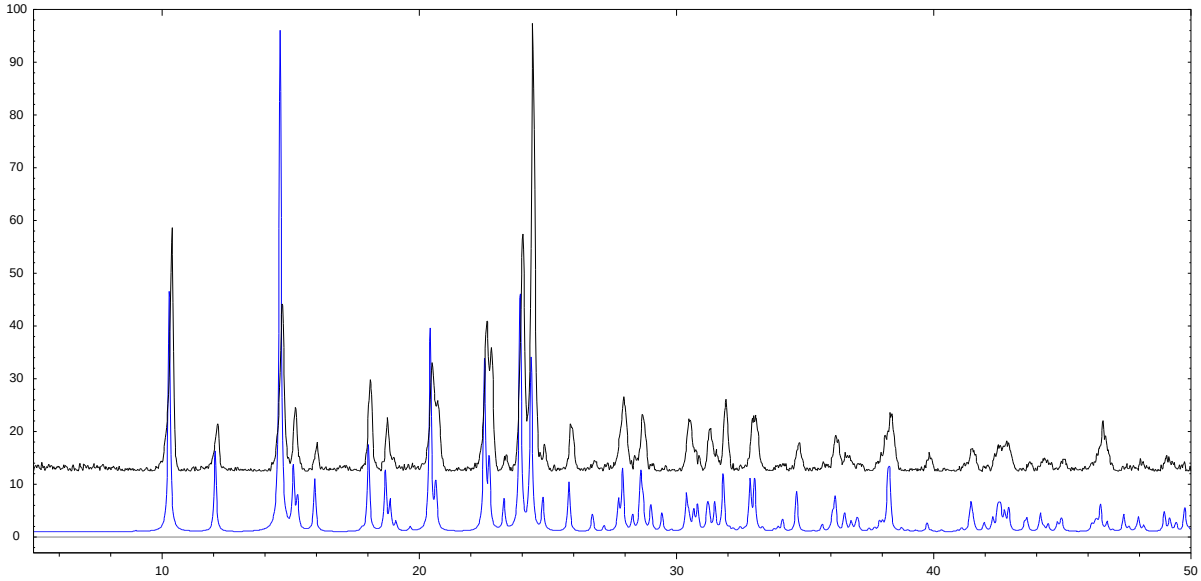

Figure S18. Experimental (**black**) and calculated (**blue**) PXRD traces of $[Co(acac)_2(2\text{-}Brpz)_2]$ (**5a**)

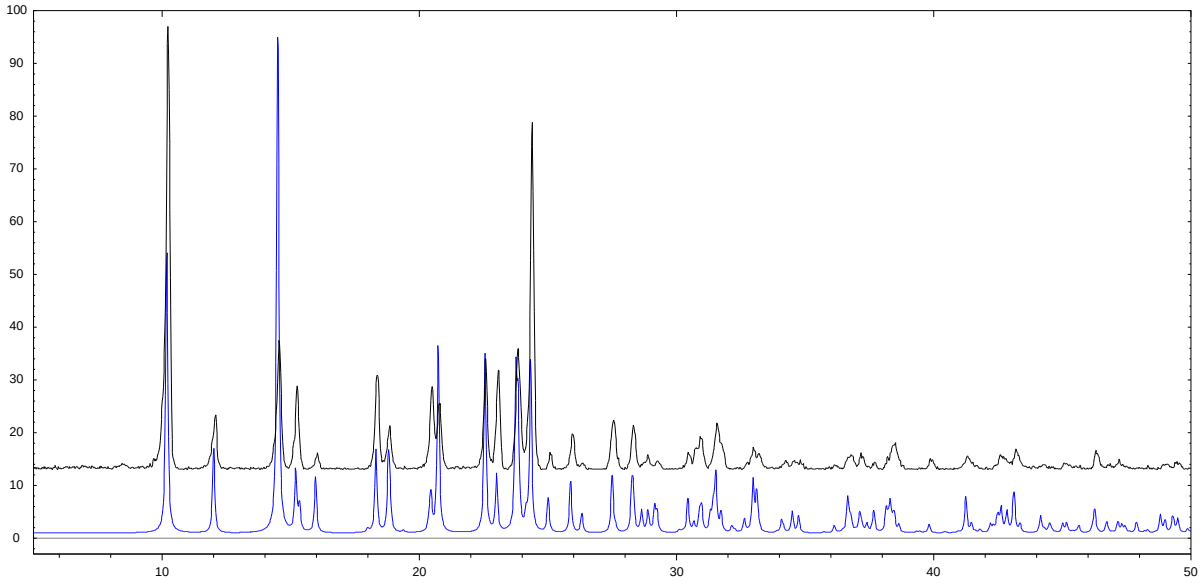

Figure S19. Experimental (**black**) and calculated (**blue**) PXRD traces of $[NI(acac)_2(2\text{-}Brpz)_2]$ (**5b**)

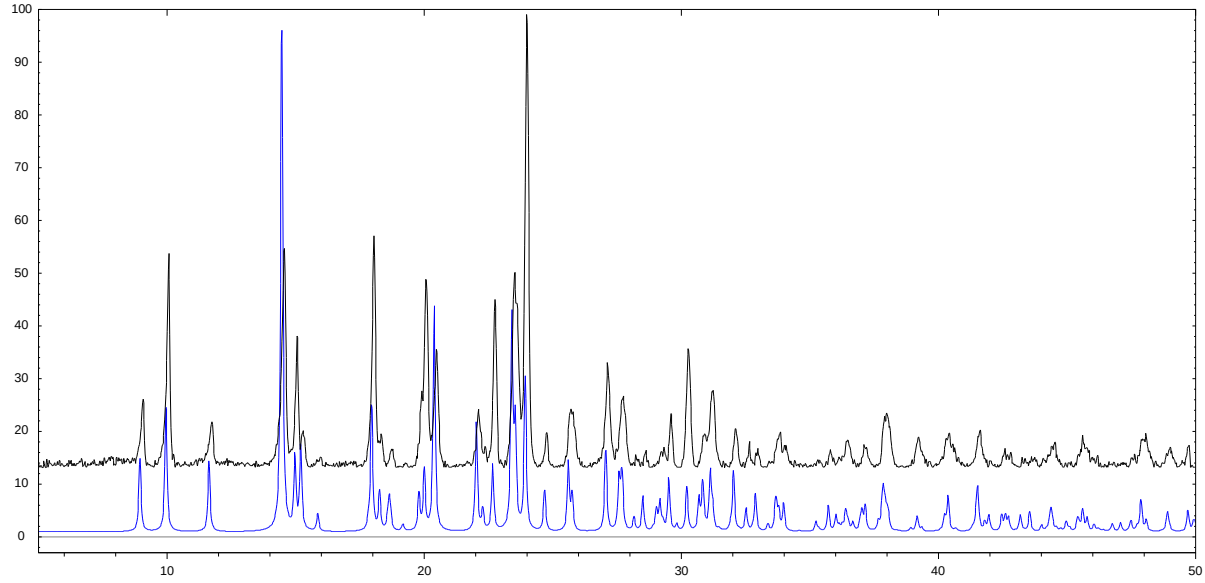

Figure S20. Experimental (black) and calculated (blue) PXRD traces of $[Co(acac)_2(2\text{-}Ipz)_2]$ (**6a**)

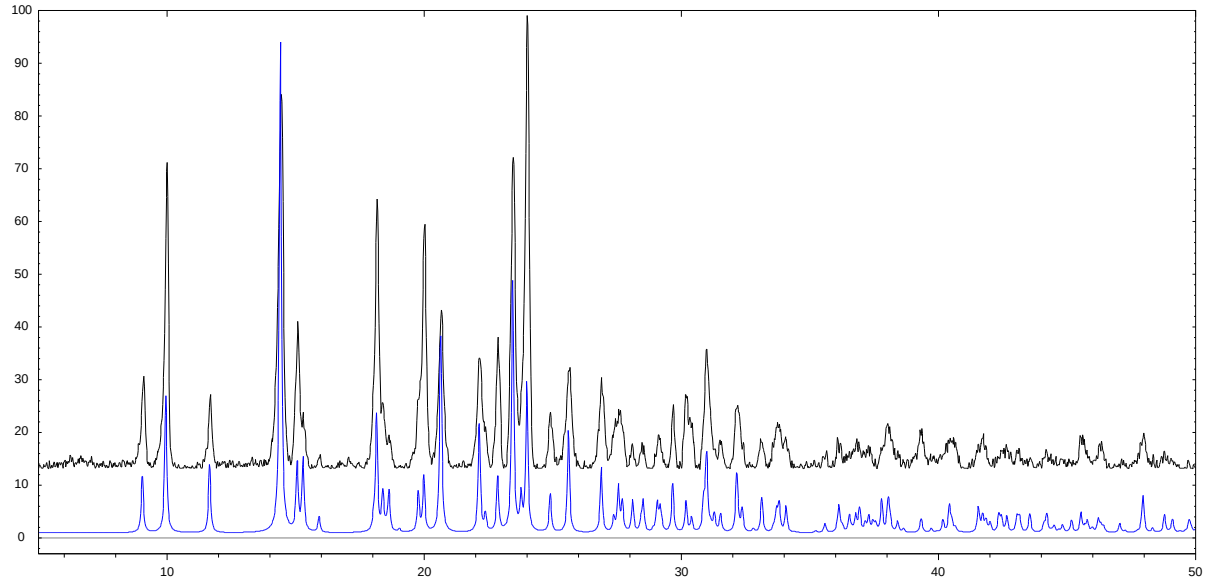

Figure S21. Experimental (**black**) and calculated (**blue**) PXRD traces of $[Ni(acac)_2(2\text{-}Ipz)_2]$ (**6b**)

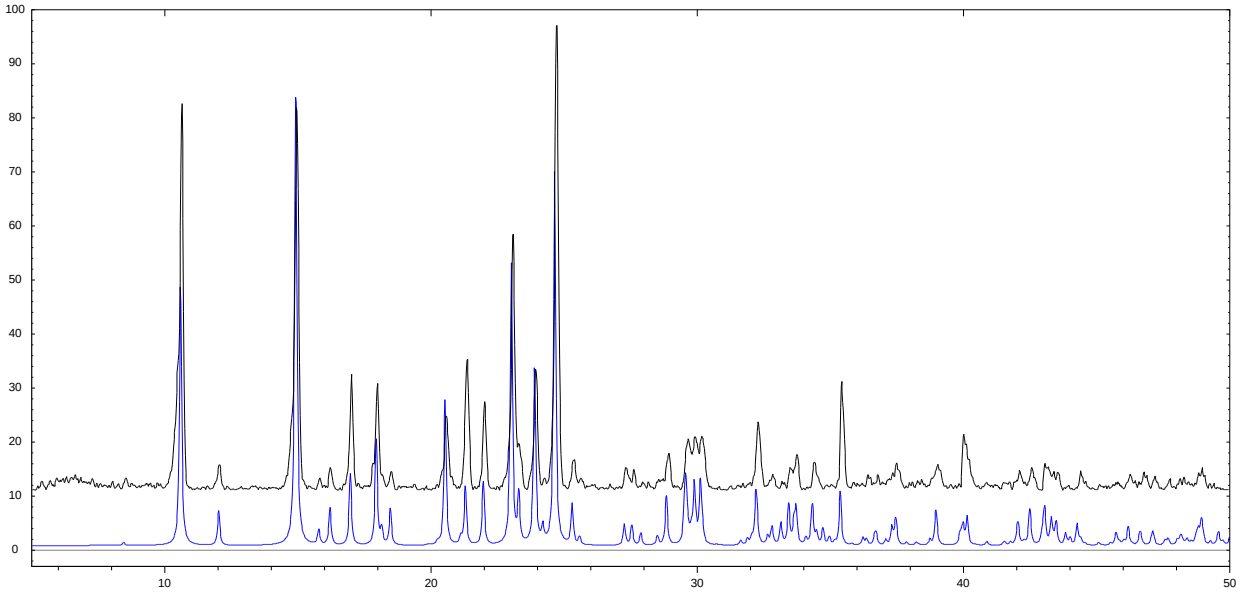

Figure S22. Experimental (**black**) and calculated (**blue**) PXRD traces of $[Co(acac)_2(5\text{-}Brpm)_2]$ (**7a**)